

February, 1981

ENERGY AND GROUP VELOCITY  
IN SEMI DISCRETIZATIONS OF  
HYPERBOLIC EQUATIONS

by

R. Vichnevetsky

DCS-TR-100

Department of Computer Science  
Rutgers University  
New Brunswick, New Jersey 08903

To appear in MATHEMATICS AND COMPUTERS IN SIMULATION  
Vo. XXIII (1981)  
North Holland Publishing Co.

Abstract

*Propagation properties of a numerical semi-discretization of hyperbolic equation are analyzed, using time-Fourier Transforms. It is shown that numerical solutions are of two types, corresponding to the two roots of a characteristic equation which is associated with the semi-discretization. The properties of those two types of solutions in terms of phase velocity, wavelength and group velocity are derived. While solutions of the first type converge to genuine solutions of the equation, solutions of the second type have group velocities opposite to the direction of flow, and are entirely spurious.*

## 1- INTRODUCTION

We analyse in this paper the propagation properties of numerical semi-discretizations of hyperbolic equations, of which

$$\frac{\partial U}{\partial t} + c \frac{\partial U}{\partial x} = 0$$

( 1 )

is taken as a simple model. The main tool used in the analysis is that of time-Fourier transforms, (the independent variable is  $t$  and the frequency  $\Omega$  has dimensions  $t^{-1}$  ).

The reason for using this tool is as follows: our ultimate objective is to analyse the spurious reflection phenomena that occur when numerical solutions pass through discontinuities such as interfaces in mesh refinement and boundaries of the computational domain. An analysis with t-Fourier transforms results in an exact analytic description of those situations.

It will be shown in the analysis that the numerical approximation of (1) by a semi discretization on a uniform mesh is described by the superposition of two types of fundamental solutions, that correspond to the same band of frequencies in the  $\hat{t}$ -Fourier domain, but that are characterized by group velocities of opposite sign. While solutions of the first type approximate exact solutions of the equation, those of the second type are entirely spurious.

The application of these mathematics to an analysis of reflection phenomena in mesh refinement is described in reference [19] that is a direct continuation of the present paper. Application to the analysis of reflection at a downstream boundary is given in [23] and at upstream boundaries in [24].

We shall consider here a regular division of the  $X$  axis:

$$x_n = n \cdot h \quad ; \quad n = \dots -2, -1, 0, 1, 2, \dots \quad (2)$$

on which (1) is approximated by the usual finite differences semi-discretization :

$$\frac{du_n}{dt} = -c \left( \frac{u_{n+1} - u_{n-1}}{2h} \right) \quad (3)$$

where

$$\{u_n(t)\} \simeq \{U(x_n, t)\}$$

is the numerical solution on the  $\hat{t}$ -continuous lines defined by (2).

(finite element semi-discretizations are examined in a separate paper, [20]).

The approximation (3) may be interpreted as that resulting from a fully

discrete algorithm, with a Courant number  $(c \cdot \Delta t / \Delta x)$  small enough that the error associated with time discretization is negligible when compared with the error associated with space discretization (in practice  $(c \cdot \Delta t / \Delta x) < .1$ ). A model such as (3) is often referred to as a "method of lines" approximation of the equation.

Since hyperbolic equations describe propagation in continuous media, it is the case that their discretizations (of which (3) is an example) describe propagation in the periodic structure obtained when a continuum is discretized and modeled by what is called a lumped parameters system. One finds

in the development of applied mathematics and physics a large and interesting succession of uses of such discrete models. One of the first is possibly that of Newton [Principia, Book II, (1686)], in his attempts to find a physical model for the propagation of sound.

In the first half of the eighteenth century, Johann and Daniel Bernoulli used similar discrete models to describe vibrating strings, and d'Alembert used this approach, passing to the limit, to "invent" (in his own words) partial differential equations.

The relation of trigonometric series with propagation in continua and in their discrete models was well known in the eighteenth century. This was used, among others, by Euler and Lagrange. The name of Fourier, that was later to be attached to those series, came when he proved that their applicability was less restricted than was believed, while he was applying them, also using discrete models at first, to solve the diffusion equation that he had just discovered.

Crystal lattices offer a physical example of a discrete conducting medium. Sinusoidal wave propagation through such structures and many of the attending developments in Fourier analysis had been well established by the end of the nineteenth century.

Many of these developments are reported in Brillouin (1946). Numerical discretizations of partial differential equations have created new families of similar periodic structures. It thus comes as no surprise that applying Fourier analysis to study their properties proves to be a very fruitful endeavor.

An important property of discrete media is that they are dispersive; that is, the phase velocity of sinusoidal waves depends on frequency. The concept of group velocity, that plays a primordial role in signal and energy propagation through dispersive media emerged in the nineteenth century. It had been used conceptually by Hamilton (1839) and by Rayleigh (Theory of Sound - 1877) but its full mathematical development came in the early part of this century with publications of Sommerfeld (1912, 1914) in prominent place. Here also, this classical result from mathematical physics provides the starting point for the investigation of a host of interesting aspects of propagation properties of numerical discretizations of hyperbolic equations.

## 2. FOURIER ANALYSIS

It shall be assumed throughout this paper that the  $\{u_n\}$  are in  $\mathcal{L}_2$ , i.e. that the  $\mathcal{L}_2$  norms:

$$\left( \int_{-\infty}^{\infty} |u_n|^2 dt \right)^{1/2} \quad (4)$$

are finite.

Let  $\{\hat{u}_n(\Omega)\}$  denote the set of time-Fourier transforms of the semi-discrete numerical solution  $\{u_n(t)\}$ :

$$\hat{u}_n(\Omega) = \int_{-\infty}^{\infty} u_n(t) \cdot e^{-i\Omega t} dt \quad (5)$$

The converse relation is:

$$u_n(t) = \int_{-\infty}^{\infty} \hat{u}_n(\Omega) \cdot e^{i\Omega t} \frac{d\Omega}{2\pi} \quad (6)$$

To analyse properties of the  $\{\hat{u}_n\}$ , we Fourier-transform equation (3) and obtain:

$$i\Omega \hat{u}_n = -c \left( \frac{\hat{u}_{n+1} - \hat{u}_{n-1}}{2h} \right)$$

or

$$\hat{u}_{n+1} + 2i \left( \frac{-\Omega h}{c} \right) \hat{u}_n - \hat{u}_{n-1} = 0 \quad (7)$$

Solving this recurrence equation may be achieved by seeking "normal" or "fundamental" solutions, i.e. solutions for which the ratio:

$$\frac{\hat{u}_{n+1}}{\hat{u}_n} \equiv \hat{E}(\Omega) \quad (8)$$

is independent of  $n$ .

We may note that  $\hat{E}(\Omega)$  is an image in the Fourier domain of the standard space-shift operator  $E$  defined by the identity.

$$u_{n+1} \equiv E \cdot u_n \quad (9)$$

To find solutions that obey (8), we insert this expression in (3) and obtain:

$$\left( \hat{E} + 2i \left( \frac{-\Omega h}{c} \right) - \hat{E}^{-1} \right) \hat{u}_n = 0 \quad (10)$$



I.e.,  $\hat{E}(\Omega)$  must satisfy the characteristic equation:

7

$$\hat{E}^2 + 2i \left( \frac{\Omega h}{c} \right) \hat{E} - 1 = 0 \quad (11)$$

This equation has the two roots (figure 1)

$$\hat{E}_1 = -i \left( \frac{\Omega h}{c} \right) + \sqrt{1 - \left( \frac{\Omega h}{c} \right)^2} \quad (12)$$

$$\hat{E}_2 = -i \left( \frac{\Omega h}{c} \right) - \sqrt{1 - \left( \frac{\Omega h}{c} \right)^2} \quad (13)$$

We shall call them "characteristic ratios" or "cell transfer functions" of the semi-discretization, borrowing the latter term from Operational Calculus (see e.g. [21])

The above leads to :

Property 1

Numerical solutions of (2) may be expressed as the sum

$$\{U_n(t)\} = \{p_n(t)\} + \{q_n(t)\} \quad (14)$$

of two fundamental types of solution. Their respective Fourier transforms:

$$\hat{p}_n(\Omega) = \hat{p}_0(\Omega) \cdot [\hat{E}_1(\Omega)]^n \quad (15)$$

and

$$\hat{q}_n(\Omega) = \hat{q}_0(\Omega) \cdot [\hat{E}_2(\Omega)]^n \quad (16)$$

describe the different propagation properties that apply to the two types,

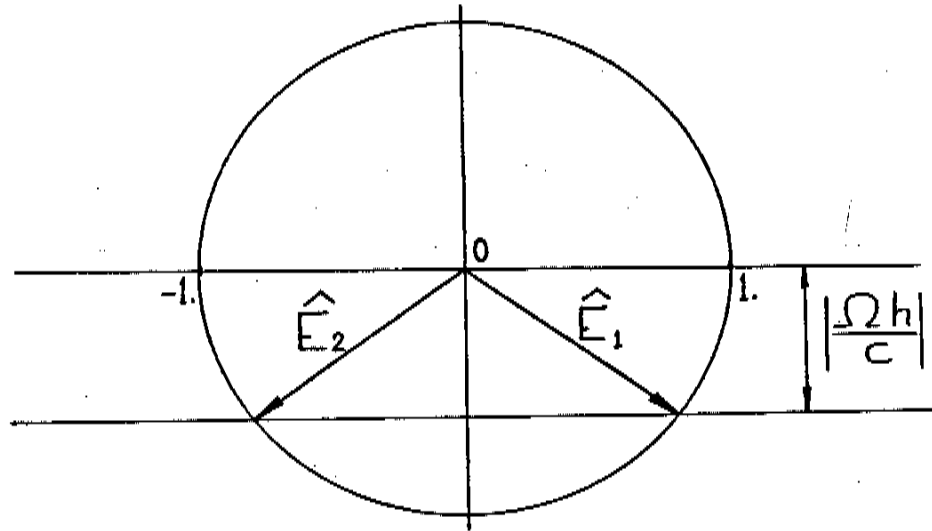


Figure 1 : Roots of the characteristic equation (16) when  $\frac{\Omega h}{c} \ll 1$

That two types of solutions may exist is a consequence of the fact that the semi-discretization (3) is a consistent approximation of the second order wave equation

$$\frac{\partial^2 U}{\partial t^2} - c^2 \frac{\partial^2 U}{\partial x^2} = 0$$

( 17)

rather than of the first order advection equation (1) (see references [16] and [17] about this).

We shall see in the sequel that to these two types of fundamental solutions correspond propagation properties that are indeed consistent approximation of the two types of characteristic solutions of (17).

3 - NUMERICAL PHASE VELOCITY AND WAVELENGTH

For comparison with (13), we express exact solutions of the advection equation also in Fourier integral form. Let:

$$\hat{U}(x, \Omega) = \int_{-\infty}^{\infty} U(x, t) \cdot e^{-i\Omega t} dt \quad (18)$$

be the time-Fourier transform of  $U$ . If  $U(x, t)$  is a solution of (1), then  $\hat{U}(x, \Omega)$  satisfies

$$i\Omega \hat{U} + c \frac{\partial \hat{U}}{\partial x} = 0$$

or, by integration:

$$\hat{U}(x, \Omega) = \hat{U}(0, \Omega) e^{-i\Omega x/c} \quad (19)$$

For each  $\Omega$  the  $x$ -dependence is harmonic (sinusoidal), with:

- a conservative amplitude

$$|\hat{U}(x, \Omega)| = |\hat{U}(0, \Omega)| \quad (20)$$

- a spatial frequency  $\omega$  given by:

$$\omega = \Omega/c \quad (21)$$

- and a wavelength

$$\lambda = 2\pi/\omega = 2\pi c/\Omega \quad (22)$$

The numerical equivalent of (19) is (15)-(16). These expressions describe different propagation properties according to whether  $(\Omega h/c)$  is  $< 1$  or  $> 1$ : The frequency:

$$\Omega_c = \frac{c}{h}$$

is a cut-off frequency. When  $\Omega > \Omega_c$ , then constant amplitude sinusoidal numerical solutions cannot exist. See reference [15] and section 4 below about this.

When  $\Omega \leq \Omega_c$ , then (15) and (16) describe fundamental solutions that are sinusoidal in space as well as in time. Indeed, we then have:

$$|\hat{E}_1(\Omega)| = |\hat{E}_2(\Omega)| = 1 \quad (23)$$

Accordingly, the amplitudes of Fourier transforms is preserved:

$$|\hat{p}_n(\Omega)| = |\hat{p}_0(\Omega) E_1^n| = |\hat{p}_0(\Omega)| \quad (24)$$

and

$$|\hat{q}_n(\Omega)| = |\hat{q}_0(\Omega) E_2^n| = |\hat{q}_0(\Omega)| \quad (25)$$

To find the corresponding numerical phase velocities, we write in a form analogous to (19):

$$\left. \begin{aligned} \hat{p}_n &= \hat{p}_0 e^{n \angle \hat{E}_1} = \hat{p}_0 e^{-i\Omega x_n / c_1^*(\Omega)} \\ \hat{q}_n &= \hat{q}_0 e^{n \angle \hat{E}_2} = \hat{q}_0 e^{-i\Omega x_n / c_2^*(\Omega)} \end{aligned} \right\} (26)$$

where

$$\angle \hat{E}_1 \equiv -\text{arc sin} (\Omega h/c) \quad (27)$$

is the phase of  $\hat{E}_1$ , and where

$$c_1^*(\Omega) = \Omega h / \text{arc sin} (\Omega h/c) \quad (28)$$

is the phase velocity at which  $\{p_n\}$  solutions propagate. The wavelength is given by the relation similar to (22):

$$\lambda_1 = \frac{2\pi c_1^*}{\Omega} = 2\pi h / \text{arc sin} (\Omega h/c) \quad (29)$$

Fundamental numerical solutions of the  $\{q_n\}$  type have a smaller phase velocity:

$$c_2^* = -\Omega h / \angle \hat{E}_2 = \Omega h / (\pi - \text{arc sin} (\Omega h/c)) \quad (30)$$

and a correspondingly shorter wavelength

$$\lambda_2 = \frac{2\pi c_2^*}{\Omega} = 2\pi h / (\pi - \text{arc sin} (\Omega h/c)) \quad (31)$$

These are illustrated in figures 2 and 3.

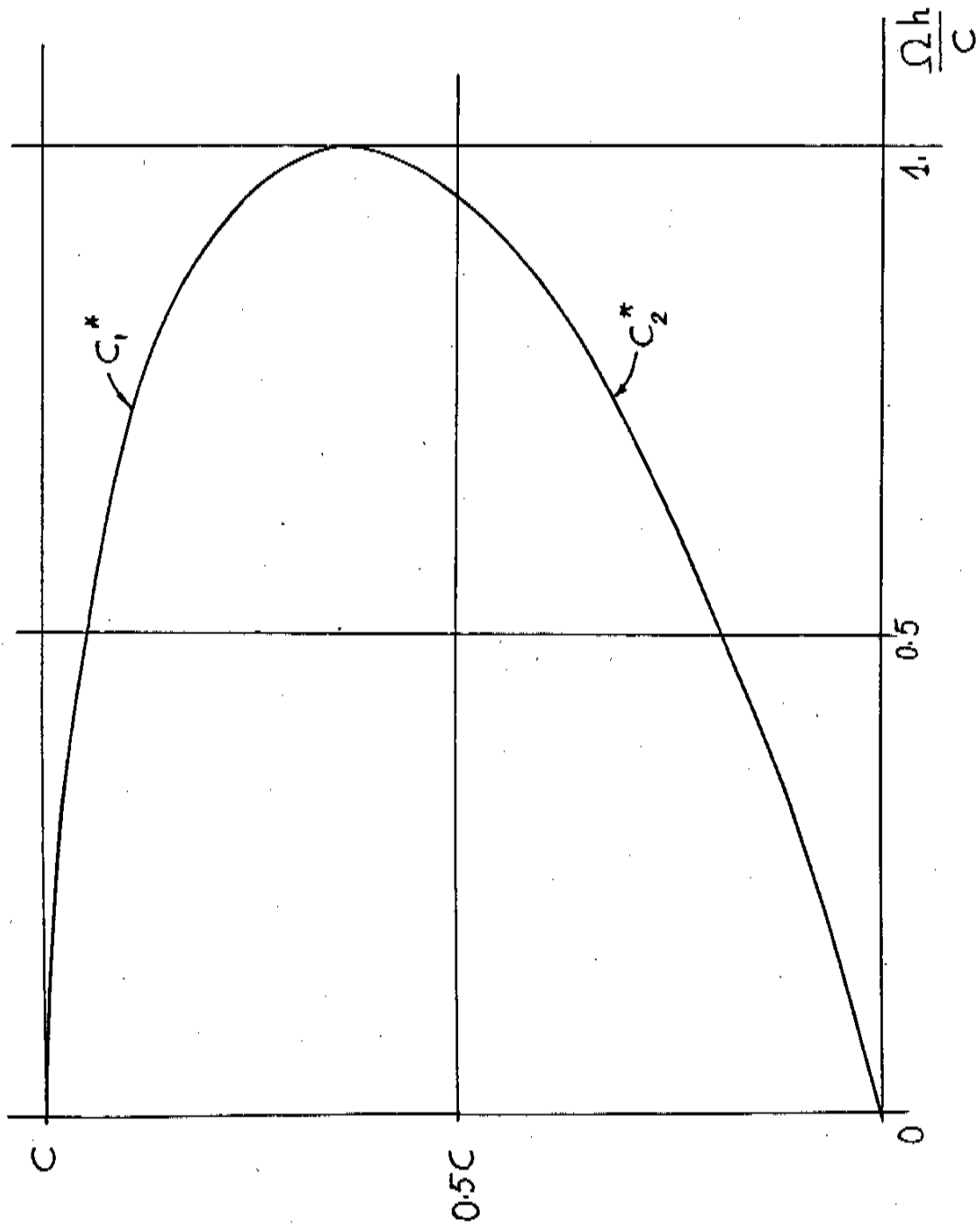


Figure 2 - Phase velocity of the semi-discretization (5)

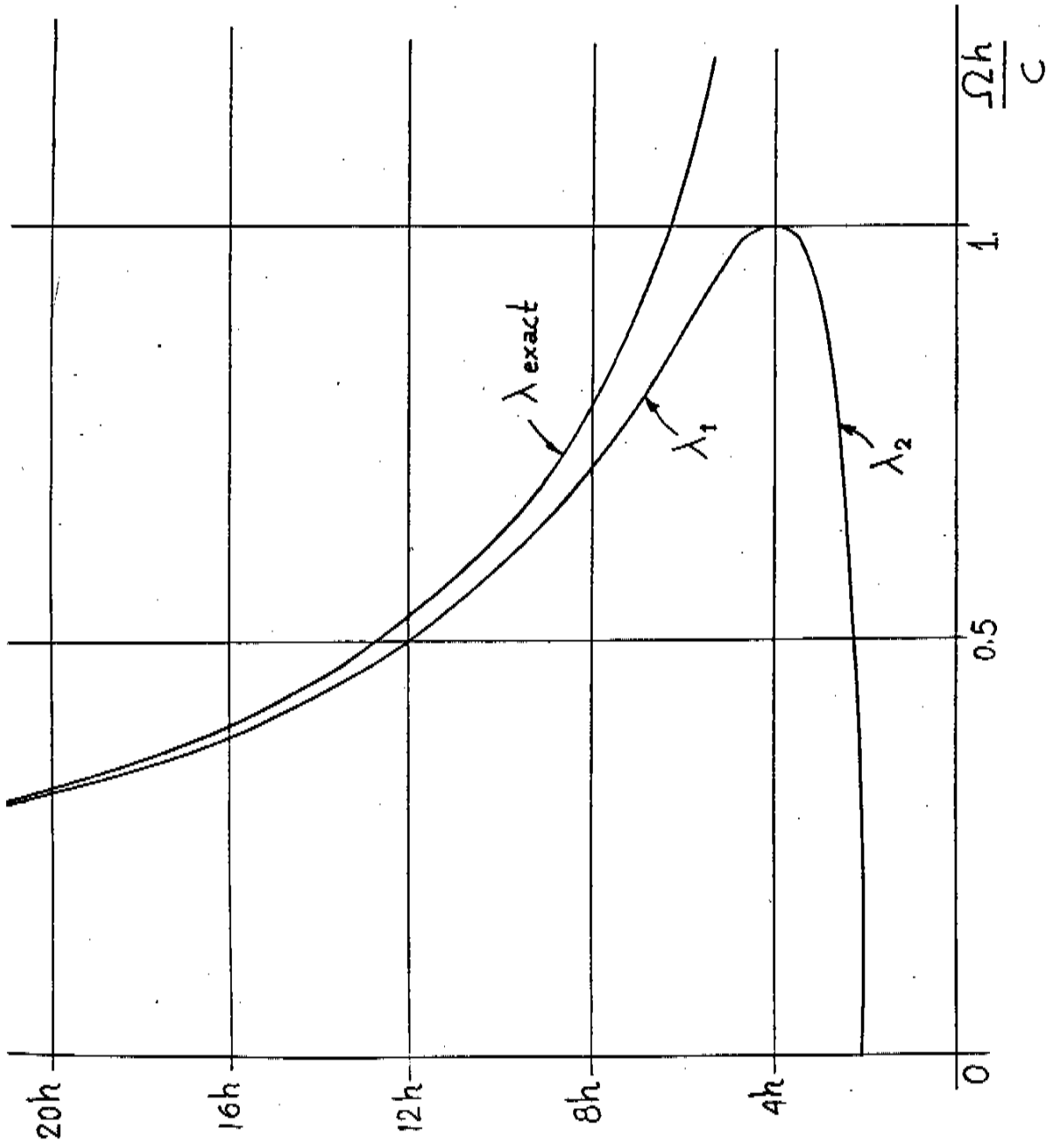


Figure 3 - Exact and numerical wavelengths corresponding to a time - frequency  $\Omega$  .



4 - CUT-OFF FREQUENCY

The situation is different when  $|\Omega h/c| > 1$ . Then the roots of the characteristic equation become (figure 4) :

$$\hat{E}_1(\Omega) = -i \left( \frac{\Omega h}{c} - \sqrt{\left(\frac{\Omega h}{c}\right)^2 - 1} \right) \quad (32)$$

$$\hat{E}_2(\Omega) = -i \left( \frac{\Omega h}{c} + \sqrt{\left(\frac{\Omega h}{c}\right)^2 - 1} \right) \quad (33)$$

Both are pure imaginary, and neither is equal to one in absolute value. We have

$$|\hat{E}_1| < 1 \quad ; \quad |\hat{E}_2| > 1$$

with

$$|\hat{E}_1| \cdot |\hat{E}_2| = 1 \quad (34)$$

Their phase is

$$\angle \hat{E}_1 = \angle \hat{E}_2 = -\frac{\pi}{2} \quad (35)$$

The corresponding "normal solutions" (equation (8)) have exponential envelopes decaying with  $\chi$  for  $\hat{E}_1$  and with  $-\chi$  for  $\hat{E}_2$

An interesting property of such solutions is that their wavelengths is equal to  $4h$  irrespectively of frequency.

Solutions of this type may occur only near boundaries, as illustrated in [15], or near other discontinuities such as in mesh refinement [19].

They cannot be generated by initial conditions on a regular mesh.

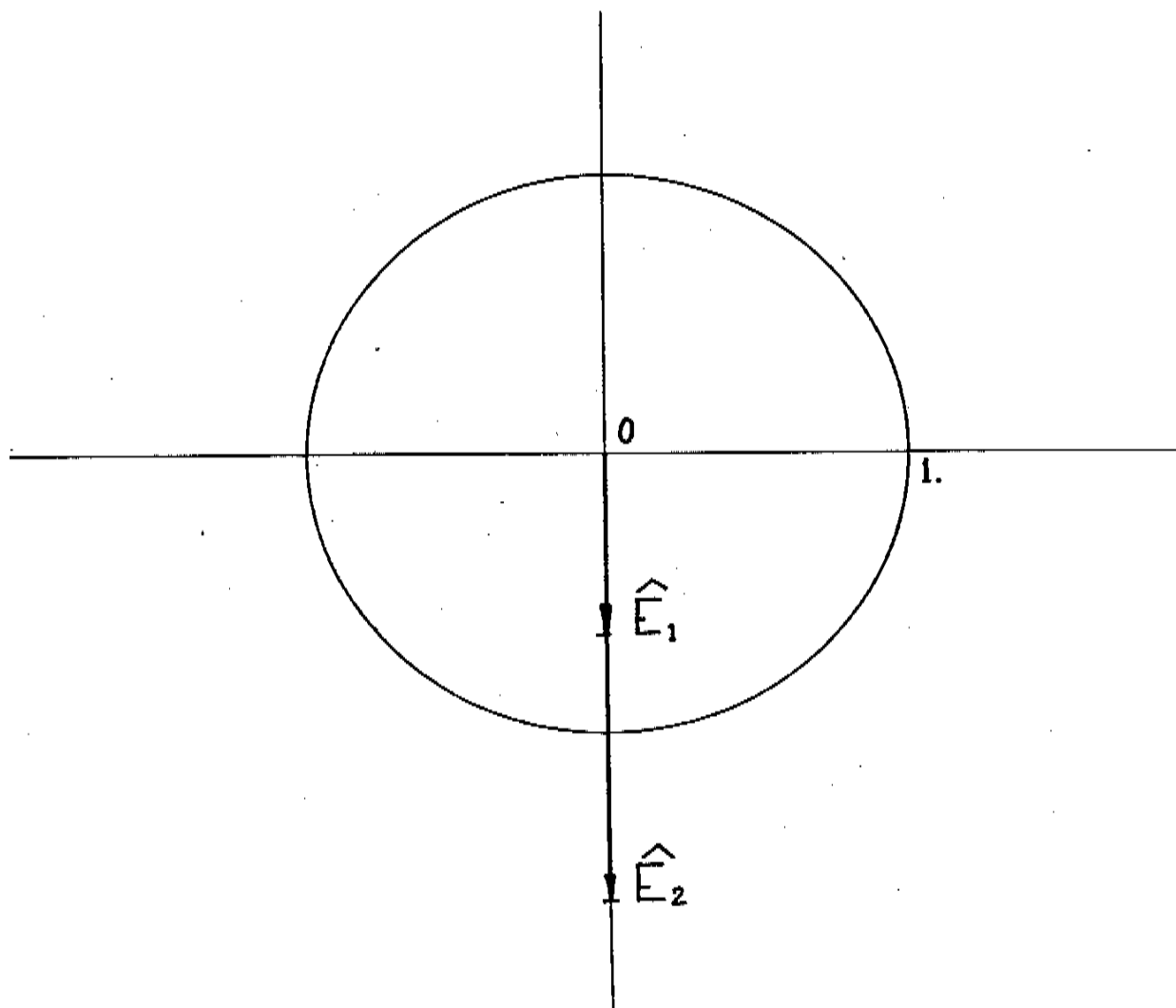


Fig. 4 - Roots of the Characteristic Equation (11)  
when  $|\Omega h/c| > 1$

### 5 - FOURIER ANALYSIS IN $\mathcal{X}$

Other aspects of propagation are obtained by using  $\mathcal{X}$ - Fourier transforms:

The usual  $\mathcal{X}$ - Fourier transform of functions  $U(x,t)$  that are in  $\mathcal{L}_2$  (meaning here that the energy

$$\int_{-\infty}^{\infty} |U(x,t)|^2 dx \equiv \|U\|_2^2 \text{ is finite) is:}$$

$$\widehat{U}(\omega, t) \equiv \int_{-\infty}^{\infty} U(x, t) \cdot e^{-i\omega x} dx \quad (36)$$

Similarly, the expression\*

$$\overline{U}(\omega, t) \equiv h \sum_{n=-\infty}^{\infty} U_n \cdot e^{-i\omega x_n} \quad (37)$$

defines the discrete Fourier transform of  $\{U_n\}$ . Here also, it is assumed that  $\{U_n\}$  is in  $\mathcal{L}_2$ , i.e. that the discrete energy, defined as

$$\|U_n\|_2^2 \equiv h \sum_n |U_n|^2 \quad (38)$$

is finite.

The correspondence between the space frequency  $\omega$  and the time frequency  $\Omega$  for numerical solutions may be obtained by using the analog of (21), viz

$$\omega = \Omega / c^*(-\Omega)$$

(39)

\* see [25] for a definition of the  $\overline{\square}$  symbol and a review of properties of discrete Fourier transforms

which, from (28) and (30) becomes

$$\begin{aligned}\omega_1 &= \Omega / c_1^*(\Omega) \\ &= \frac{1}{h} \arcsin(\Omega h / c) \leq \frac{\pi}{2h}\end{aligned}\quad (40)$$

$$\begin{aligned}\omega_2 &= \Omega / c_2^*(\Omega) \\ &= \frac{1}{h} (\pi - \arcsin(\Omega h / c)) \geq \frac{\pi}{2h}\end{aligned}\quad (41)$$

The converse relation

$$\Omega = \frac{c}{h} \cdot \sin(\omega h) \quad (42)$$

holds for both types of fundamental solutions.

The domains in which  $\omega$  and  $\Omega$  take their values are  $[-\pi/h, \pi/h]$  and  $[-c/h, c/h]$  respectively. The correspondence is not one-to-one, but two-to-one, viz. (figure 5):

for solutions of  $\{p_n\}$  type:

$$|\omega| \in [0, \frac{\pi}{2h}] \rightarrow |\Omega| \in [0, \frac{c}{h}] \quad (43)$$

for solutions of  $\{q_n\}$  type:

$$|\omega| \in [\frac{\pi}{2h}, \frac{\pi}{h}] \rightarrow |\Omega| \in [\frac{c}{h}, 0] \quad (44)$$

We may observe from this that:

Property 2:

The  $x$ -Fourier transforms of fundamental solutions of the  $\{p_n\}$  and  $\{q_n\}$  type have non overlapping support in  $\omega$ :

$$0 \leq \omega_1 \leq \frac{\pi}{2h} \leq \omega_2 \leq \pi \quad (45)$$

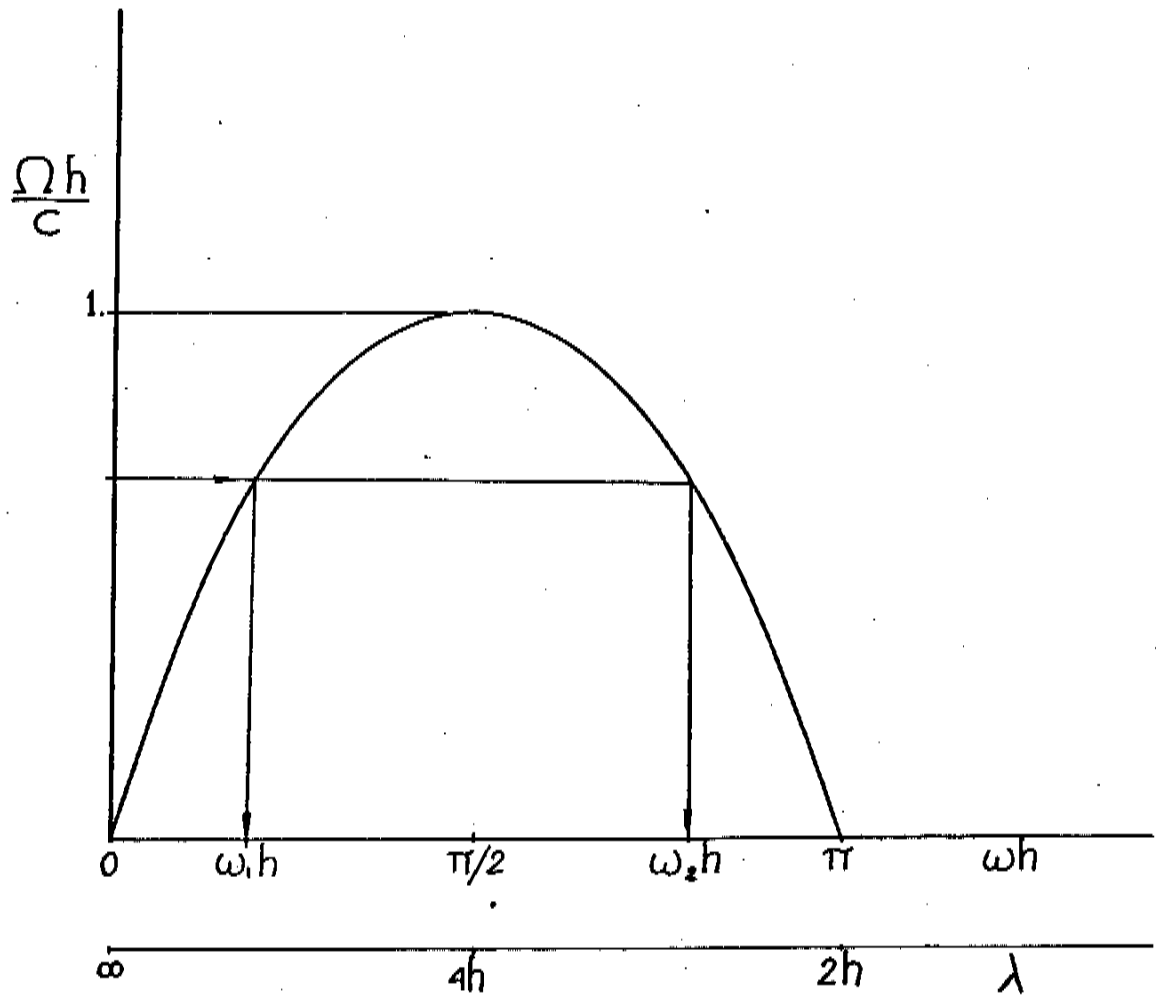


FIGURE 5: To each time frequency  $\Omega < \frac{h}{c}$  correspond two space frequencies  $\omega_1$  and  $\omega_2$ , characterizing fundamental solutions of  $\{p_n\}$  and  $\{q_n\}$  type, respectively

The analog of this separation principle in terms of wavelengths may be stated as, from (29) and (31): -(see also figure 3)

Property 3:

Numerical solutions of the  $\{p_n\}$  type have

Fourier components with wavelengths  $\lambda_1$  in  $(4h, \infty)$

while numerical solutions of the  $\{q_n\}$  type have Fourier components with wavelengths  $\lambda_2$  in  $(2h, 4h)$ .

This property explains the well documented observation that spurious reflections of numerical solutions is always associated with short wavelengths. It is shown elsewhere (see e.g. [19] and [23]) that those spurious reflections consist of solutions of  $\{q_n\}$  type and that therefor they have wavelengths  $\lambda_2$  between  $2h$  and  $4h$  (By contrast, a similar analysis for linear finite element semi-discretizations - in [20] - will show that solutions of  $\{q_n\}$  type have wavelengths that are restricted in that case to the smaller interval  $2h \leq \lambda_2 \leq 3h$ ).

Phase velocities in terms of  $\omega$  may be derived from (40):

$$\begin{aligned}\omega &= \frac{1}{h} \arcsin(\Omega h/c) \\ &= \frac{1}{h} \arcsin(\omega h c^*/c)\end{aligned}$$

which gives the known result:

$$c^*(\omega) = c \cdot \frac{\sin(\omega h)}{\omega h} \quad (46)$$

that holds for both types of fundamental solutions.

An important property of solutions of hyperbolic equations is that they obey an energy conservation principle. I.e., if  $U(x,t)$  is a solution of the advection equation (1), then

$$\begin{aligned} \frac{d}{dt} \|U\|_2^2 &= 2 \int U \frac{\partial U}{\partial t} dx \\ &= -2 \int c U \frac{\partial U}{\partial x} dx \\ &= [-c U^2]_{-\infty}^{+\infty} \end{aligned} \quad (47)$$

The assumption that  $U$  is in  $\mathcal{L}_2$  implies that  $U(\pm\infty, t) = 0$ , and therefore that the above vanishes. Thus:

$$\|U\|_2^2 = \text{constant} \quad (48)$$

It may be observed that energy conservation is preserved by the semi-discretization (2). Indeed, multiplying (2) by  $U_n$  and summing over all  $n$  results in:

$$\begin{aligned} \frac{d}{dt} \|U_n\|_2^2 &= 2h \sum_n U_n \frac{dU_n}{dt} \\ &= -c \sum_n U_n (U_{n+1} - U_{n-1}) \\ &= -c [U_n \cdot U_{n+1}]_{-\infty}^{+\infty} \end{aligned} \quad (49)$$

The assumption that  $\{U_n\}$  is in  $\mathcal{L}_2$  implies that  $|U_{\pm\infty}| = 0$ , whence that:

$$\|U_n\|_2^2 = h \sum_n |U_n|^2 = \text{constant} \quad (50)$$

The energy of  $U$  may be expressed in terms of its Fourier transform  $\hat{U}(\omega, t)$  through Parseval's relation as:

$$\|U\|_2^2 = \int_{-\infty}^{+\infty} |\hat{U}(\omega, t)|^2 \frac{d\omega}{2\pi} \quad (51)$$

Conservation of energy results here from the fact that:

$$\frac{\partial}{\partial t} |\hat{U}(\omega, t)| = 0 \quad (52)$$

for solutions of the advection equation (1).

The energy of the discrete function  $\{u_n\}$  is expressed by the appropriate form of Parseval's relation as (see [14] or [23] for a detailed description):

$$\begin{aligned} \|u_n\|_2^2 &= \int_{-\frac{\pi}{h}}^{\frac{\pi}{h}} |\bar{u}(\omega, t)|^2 \frac{d\omega}{2\pi} \\ &= \int_0^{\frac{\pi}{h}} |\bar{u}(\omega, t)|^2 \frac{d\omega}{\pi} \end{aligned} \quad (53)$$

The discrete Fourier transform  $\bar{u}$  is decomposed in its two components:

$$\bar{u}(\omega, t) = \bar{p}(\omega, t) + \bar{q}(\omega, t) \quad (54)$$

Then, from

$$\|p_n\|_2^2 = \int_0^{\frac{\pi}{h}} |\bar{p}(\omega, t)|^2 \frac{d\omega}{\pi} = \int_0^{\frac{\pi}{2h}} |\bar{p}(\omega, t)|^2 \frac{d\omega}{\pi} \quad (55)$$

and

$$\|q_n\|_2^2 = \int_0^{\frac{\pi}{h}} |\bar{q}(\omega, t)|^2 \frac{d\omega}{\pi} = \int_{\frac{\pi}{2h}}^{\frac{\pi}{h}} |\bar{q}(\omega, t)|^2 \frac{d\omega}{\pi} \quad (56)$$

results the simple and interesting energy separation property:

Property 4

The energy of numerical solutions  $\{u_n\} = \{p_n\} + \{q_n\}$  satisfies the separation principle

$$\|u_n\|_2^2 = \|p_n\|_2^2 + \|q_n\|_2^2 \quad (57)$$



## 7 - ENERGY PROPAGATION AND GROUP VELOCITY

To study energy propagation in numerical solutions, we introduce the concepts of "wave group" or "wave packet" as they are used in classical physics.

It is by analyzing the propagation of wave packets in dispersive media that the concept of group velocity appears: A dispersive medium is one where sinusoidal functions are propagated without amplitude decay, at a phase velocity  $c^*(\omega)$  that is frequency dependent.

That is, propagation is described by:

$$V(x,t) = \int \hat{V}(\omega,0) e^{i\omega(x - c^*(\omega)t)} \frac{d\omega}{2\pi} \quad (59)$$

A "wave packet" is a single frequency sinusoidal function modulated by a slowly varying envelope as illustrated in figure 6. The mathematical description of a wave packet of frequency  $\beta$  at some initial time  $t=0$  is

$$V(x,0) = A(x,0) e^{i\beta x} \quad (59)$$

If the Fourier transform of the envelope  $A(x,0)$  is  $\hat{A}(\omega,0)$ , the assumption that  $A$  varies slowly is equivalent to assuming that  $\hat{A}$  is band limited:

$$\hat{A}(\omega,0) = 0 \quad \text{when} \quad |\omega| > \gamma \quad ; \quad \gamma \ll \beta$$

(60)

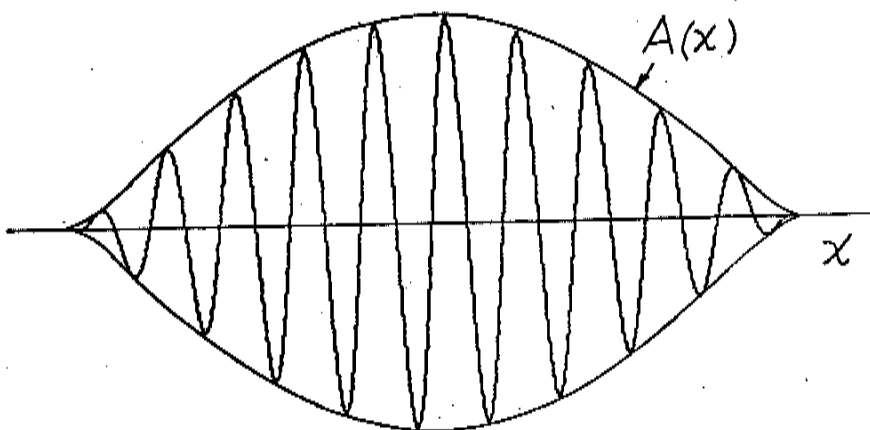


**Figure 6:** Typical wave packet, consisting of short wavelengths oscillations modulated by a slowly varying envelope.

The Fourier transform of ( 59 ) is obtained by the convolution rule :

$$\begin{aligned}\hat{V}(\omega, 0) &= \hat{A}(\omega, 0) \otimes 2\pi \delta(\omega - \beta) \\ &= \int \hat{A}(\alpha, 0) \cdot 2\pi \delta(\alpha - \omega + \beta) \frac{d\alpha}{2\pi} \\ &= \hat{A}(\omega - \beta)\end{aligned}\quad (61)$$

Applying then (58) to find the time-history of  $V(x, t)$ , we obtain:

$$V(x, t) = \int \hat{A}(\omega - \beta) \cdot e^{i\omega(x - c^*(\omega)t)} \frac{d\omega}{2\pi}$$

Since, from (60), the integrand is non zero only in the narrow band  $\omega \in (\beta - \gamma, \beta + \gamma)$ , we may use Taylor's theorem to rewrite the above as

$$\begin{aligned}V(x, t) &= \\ &\int \hat{A}(\omega - \beta) e^{i\omega x} e^{-i(\beta c^*(\beta) + (\omega - \beta) \gamma(\beta))t} \frac{d\omega}{2\pi}\end{aligned}\quad (62)$$

where

$$\gamma(\omega) = \frac{d}{d\omega} (\omega c^*(\omega))\quad (63)$$

This expression for  $V(x,t)$  may now be rewritten as :

$$\begin{aligned}
 V(x,t) &= \int \hat{A}(\omega-\beta) e^{i(\omega-\beta)(x-\mathcal{V}(\beta)t)} \cdot e^{i\beta(x-c^*(\beta)t)} \frac{d\omega}{2\pi} \\
 &= A(x-\mathcal{V}(\beta)t) e^{i\beta(x-c^*(\beta)t)} \quad (64)
 \end{aligned}$$

which expresses that the wave packet propagates as:

- a sinusoidal function of frequency  $\beta$ , moving without distortion at the phase velocity  $c^*(\beta)$

-modulated by an envelope  $A(x-\mathcal{V}(\beta)t)$  moving without distortion at the velocity  $\mathcal{V}(\beta)$ , called the group velocity.

The energy of the wave packet

$$\int |A(x-\mathcal{V}t) \cdot e^{i\omega(x-c^*t)}|^2 dx = \int |A(x,t)|^2 dx \quad (65)$$

is constant. This energy, which is concentrated in the wave packet, thus travels with the packet at the group velocity  $\mathcal{V}(\beta)$ : the group velocity is also the velocity at which energy is propagated in the dispersive medium.

The group velocity  $v$  may also be derived from  $c^*(\Omega)$ . Since

$$v = \frac{d}{d\omega} (\omega c^*(\omega)) = \frac{d\Omega}{d(\Omega/c^*(\Omega))} \quad (66)$$

we find

$$\frac{1}{v(\Omega)} = \frac{d}{d\Omega} \left( \frac{\Omega}{c^*(\Omega)} \right) \quad (67)$$

8 - GROUP VELOCITY OF NUMERICAL SOLUTIONS

If we apply these results to analyze properties of numerical solutions of the advection equation where  $C^*$  is given by (28) and (30), then we find :

$$\frac{1}{\mathcal{V}_1} = \frac{d}{d\Omega} \left( \frac{\Omega}{C_1^*(\Omega)} \right) = \frac{1}{c \sqrt{1 - (\Omega h/c)^2}}$$

or

$$\mathcal{V}_1 = c \sqrt{1 - (\Omega h/c)^2} \quad (69)$$

and

$$\frac{1}{\mathcal{V}_2} = \frac{d}{d\Omega} \left( \frac{\Omega}{C_2^*(\Omega)} \right) = \frac{-1}{c \sqrt{1 - (\Omega h/c)^2}}$$

or

$$\mathcal{V}_2 = -c \sqrt{1 - (\Omega h/c)^2} \quad (69)$$

These functions are illustrated in figure 7.

While to the fundamental solution  $\{p_n\}$  corresponds a positive group velocity  $\mathcal{V}_1$ , we observe that the group velocity  $\mathcal{V}_2$  of the fundamental solution  $\{q_n\}$  is negative. The envelope of solutions characterized by  $\{q_n\}$ , and the energy carried by such solutions, thus travels backward -

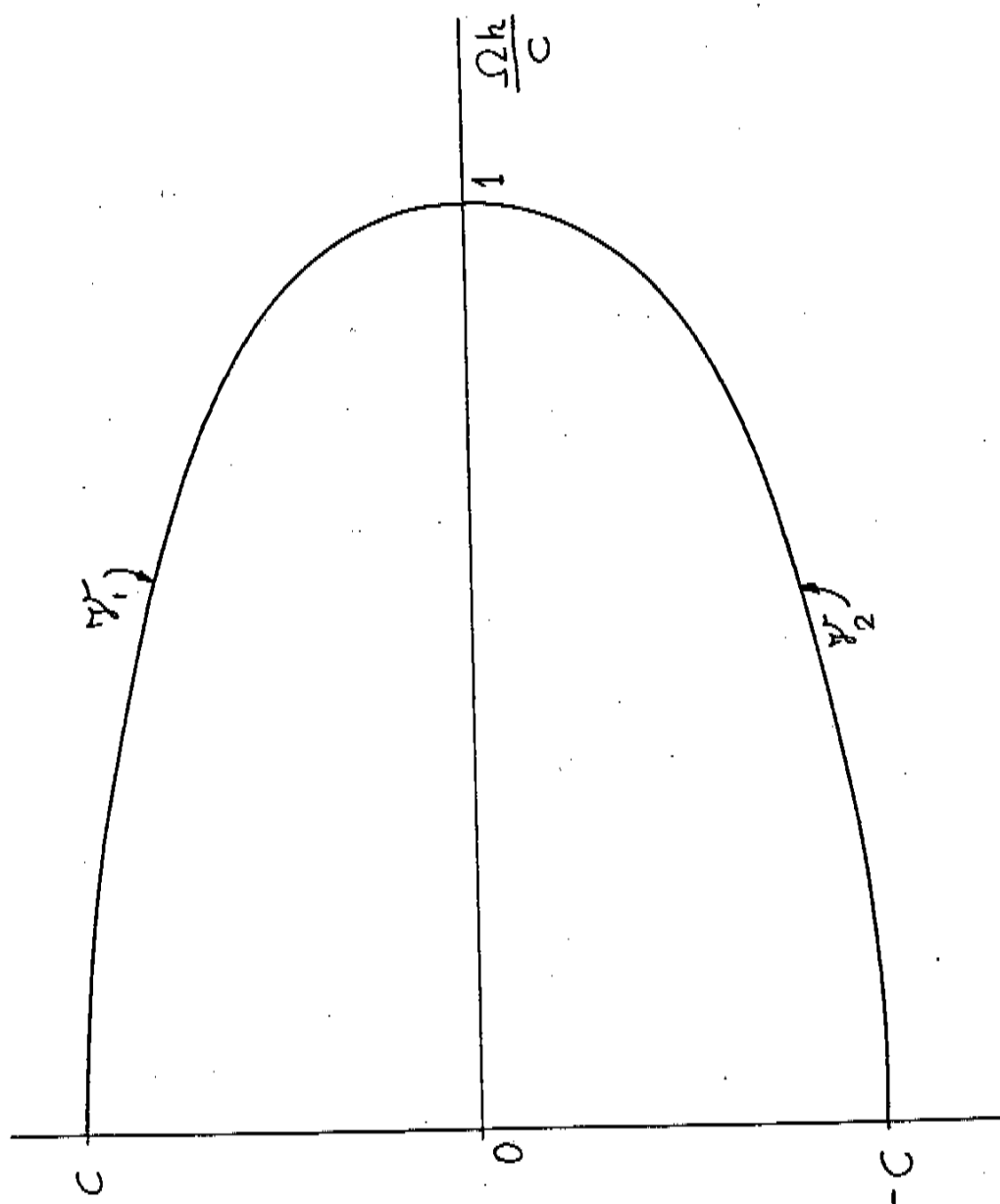


Figure 2 = Group velocity of the finite -  
difference semi-discretization (3).

The expression of the group velocity of numerical solutions as a function of  $\omega$  may be derived by applying (63) to (46) :

$$v_g = \frac{d}{d\omega} (\omega \cdot c^*(\omega)) = c \cdot \cos(\omega h)$$

which holds for both types of fundamental solutions

We may observe that, as expected,  $v_g$  is positive for  $|\omega|$  in  $[0, \frac{\pi}{2h}]$  (corresponding to fundamental solutions of the  $\{p_n\}$  type) and is negative beyond.



This may be expressed as

Property 5

A numerical wave packet of the  $\{p_n\}$  type (i.e., of wavelength  $\lambda_1 > 4h$  or frequency  $\omega_1 < \pi/2h$ ) has a positive group velocity. For smooth numerical solutions,

$(\omega h \rightarrow 0 \text{ or } \frac{\lambda}{h} \rightarrow \infty)$  this group velocity approaches  $+c$ .

Smooth numerical solutions converge to the exact solution of (1), with both group and phase velocity approaching the exact value  $+c$ .

Property 6

A numerical wave packet of the  $\{q_n\}$  type (i.e., of wavelength in the interval  $2h > \lambda > 4h$ ) has a negative group velocity - For the highest frequency ( $\omega = \frac{\pi}{h}$  or  $\lambda = 2h$ ) this group velocity equals  $-c$ .

Such ( $\lambda = 2h$ ) wave packets are consistent approximations of solutions of the spurious part:

$$\frac{\partial U}{\partial t} - c \frac{\partial U}{\partial x} = 0 \quad (70)$$

of the wave equation (17). (The existence and properties of such backward travelling wave packets was first demonstrated in [16].)

The 2 fundamental cases are illustrated in the numerical experiments shown in figure 8 A, B and C.

We note in passing that the limit cases  $\omega=0$  and  $\omega = \pi/h$  both correspond to the same time frequency  $\Omega = 0$

We also note that the phase velocities  $C_1^*$  and  $C_2^*$  of both fundamental solutions are positive. But, as shown, solutions of the  $\{q_n\}$  type have an envelope and energy that is carried backward, from right to left.

Since solutions of the  $\{p_n\}$  and  $\{q_n\}$  type carry energy forward and backward respectively, it is convenient to refer to  $\{p_n\}$  as "forward solutions" and to  $\{q_n\}$  as "backward solutions".

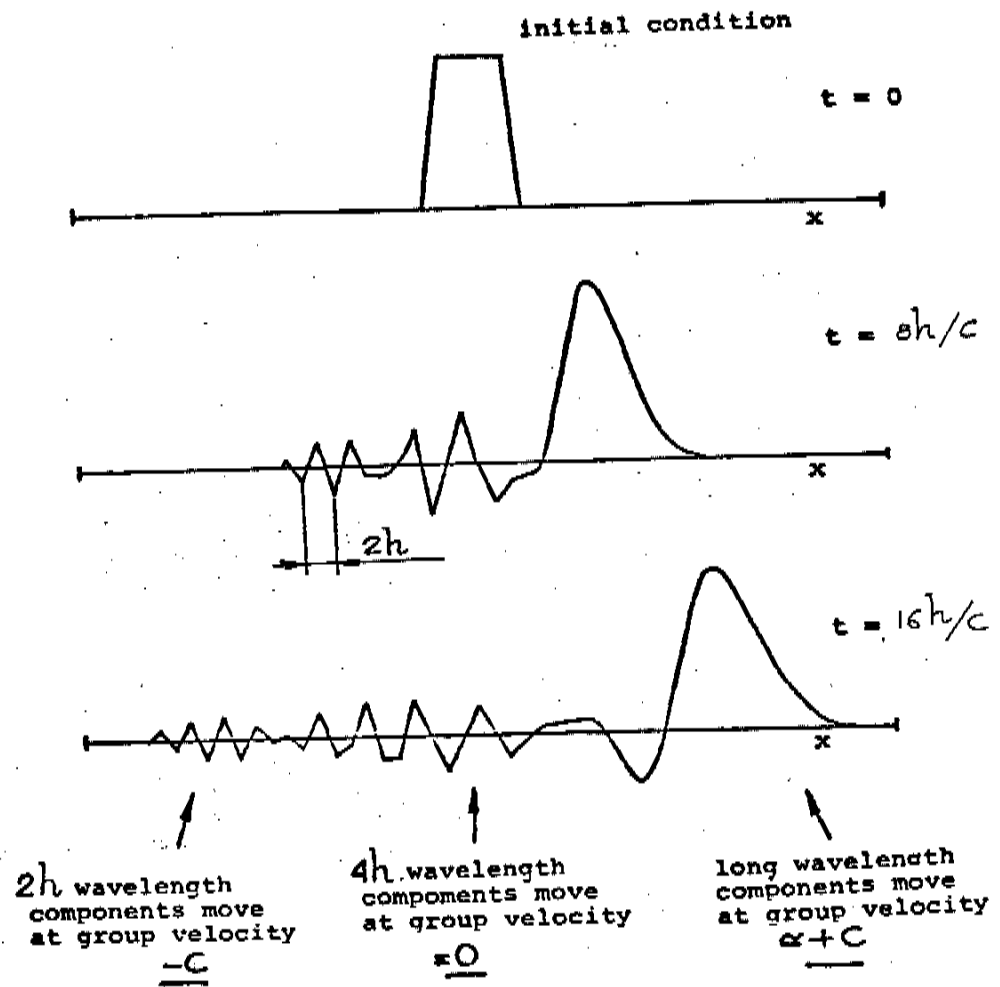


Figure 8 A

An initial condition that is mostly of  $\{p_n\}$  type is decomposed by the numerical computation into its different components.

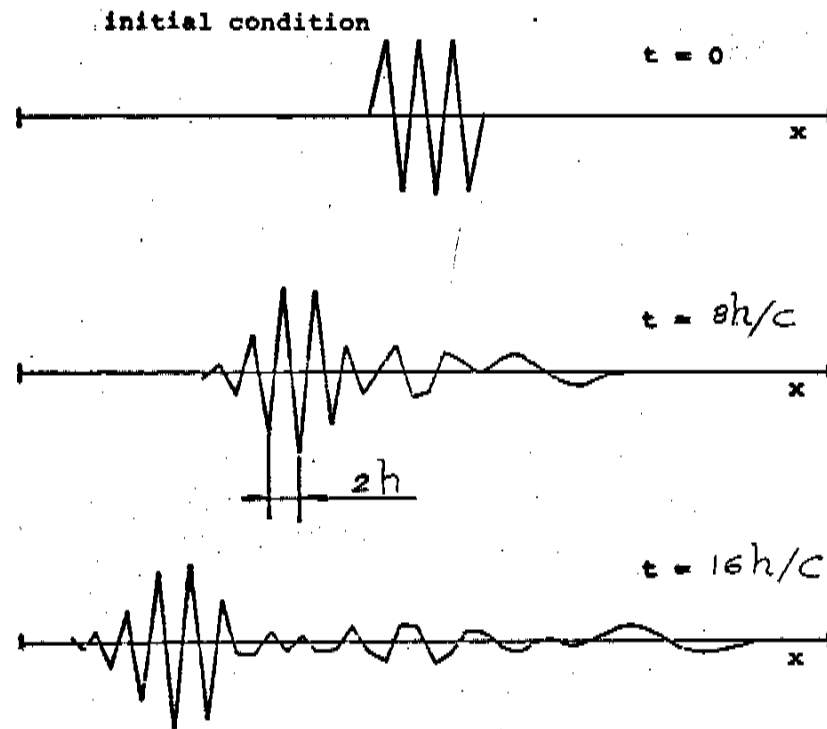


Figure 8B An initial function that is mostly of  $\{q_n\}$  type has an envelope that propagates at the predicted group velocity

$$\mathcal{V}\left(\frac{\pi}{h}\right) \approx -c$$

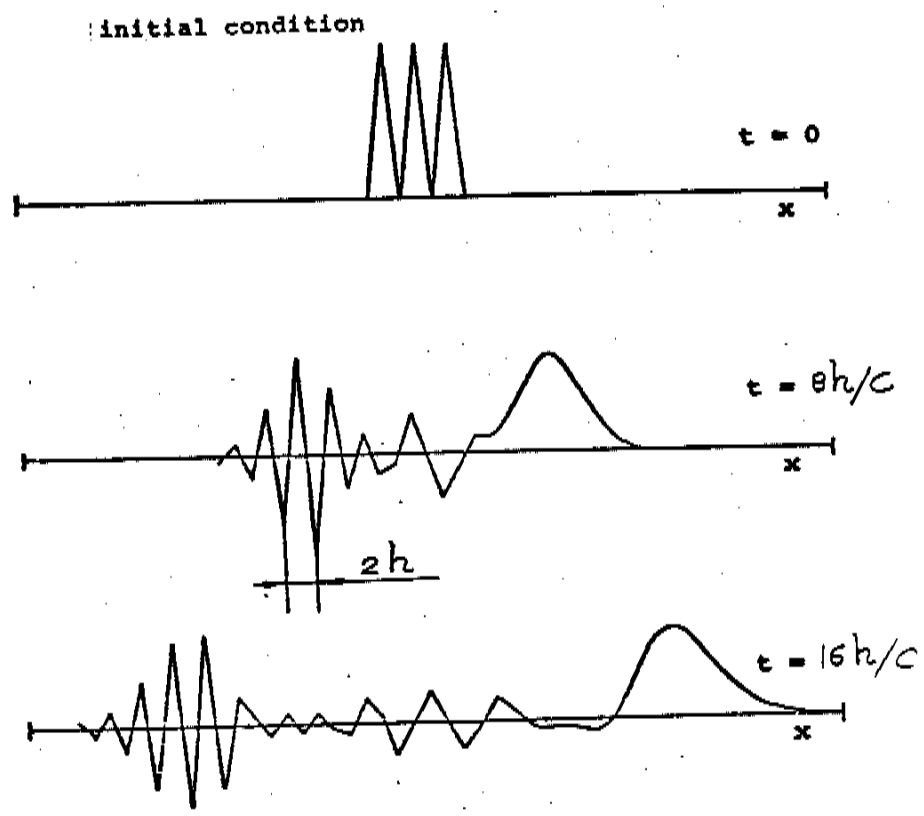


Figure 8 C - Superposition of the two preceding cases - The numerical results illustrate the separation of the solutions of  $\{p_n\}$  and  $\{q_n\}$  type that are present in the initial function.

### 9 - ENERGY FLOW

For a function  $V(x, t)$  that has constant energy, the energy flow  $\Phi(x, t)$  through a point  $x = x_A$  is defined as the rate at which energy passes from  $x < x_A$  to  $x > x_A$

If  $\{u_n\}$  is a numerical wave packet of frequency

$$\beta < \frac{\pi}{2h} \quad (\text{i.e. } \{u_n\} = \{p_n\} + 0)$$

and of finite support in  $x$ , then, for some  $T_1, T_2$  and  $x_A$ , the energy of  $\{u_n\}$  is entirely contained:

$$\left. \begin{array}{l} - \text{ in } x < x_A \quad \text{for } t < T_1 \\ - \text{ and in } x > x_A \quad \text{for } t > T_2 \end{array} \right\} \quad (71)$$

Thus, expressing the passage of the energy contained in  $\{u_n\}$  through the point  $x = x_A$  results in:

$$\int_{-\infty}^{\infty} \Phi(x, t) dt = \|p_n\|_2^2 \quad (72)$$

where the right hand side (a constant) may be evaluated at any time  $t$

Since energy flow is equal to local energy density times group velocity, this may also be expressed, from previous results, as:

$$\int_{-\frac{c}{h}}^{\frac{c}{h}} \mathcal{V}(\beta) |\hat{p}_A(\Omega)|^2 \frac{d\Omega}{2\pi} = \mathcal{V}(\beta) \int_{-\frac{c}{h}}^{\frac{c}{h}} |\hat{p}_A(\Omega)|^2 \frac{d\Omega}{2\pi} \\ = \|p_n\|_2^2 \quad (73)$$

Likewise, for any numerical solution that satisfies (71), that is not a wave packet but that consists of a  $\{p_n\}$  component only, the flow of energy through the point  $x = x_A$  is expressed by:

$$\int_{-\frac{c}{h}}^{\frac{c}{h}} \mathcal{V}(\Omega) |\hat{p}_A(\Omega)|^2 \frac{d\Omega}{2\pi} = \|p_n\|_2^2 \quad (74)$$

Since

$$d\Omega = \mathcal{V} d\omega \quad (75)$$

we may also write:

$$\int_{-\frac{\pi}{2h}}^{\frac{\pi}{2h}} |\mathcal{V}(\Omega) \hat{p}_A(\Omega)|^2 \frac{d\omega}{2\pi} = \|p_n\|_2^2 \\ = \int_{-\frac{\pi}{2h}}^{\frac{\pi}{2h}} |\bar{p}(\omega, t)|^2 \frac{d\omega}{2\pi} \quad (76)$$

From this we may derive a relationship between the amplitude of the  $t$ -Fourier transform and  $X$ -Fourier transform:

$$|\overline{P}(\omega, t)| = |\hat{P}_s(\Omega) \cdot \mathcal{Y}_i(\Omega)| \quad (77)$$

where  $\omega$  and  $\Omega$  are related by (39)



REFERENCES

- [1] Birkhoff, G. and V. A. Dougalis (1975)  
 "Numerical Solution of Hydrodynamic Problems"-  
 in ADVANCES IN COMPUTER METHODS FOR PARTIAL  
 DIFFERENTIAL EQUATIONS - R. Vichnevetsky (ed.)  
 pub. AICA, New Brunswick, N.J.
- [2] Brillouin, L. (1946)  
 "Wave Propagation in Periodic Structures"  
 McGraw Hill, New York
- [3] Brillouin, L. (1960)  
 "Wave Propagation and Group Velocity"  
 Academic Press Inc., New York, New York
- [4] Carver, M. B. and H. W. Hinds (1978)  
 "The Method of Lines and The Advective Equation"-  
 SIMULATION - Vol. 31, pp. 59-69
- [5] Carver M.B. and W.E.Schiesser (1980) " Biased  
 upwind difference approximations for first order  
 hyperbolic partial differential equations".  
 73d. Annual Meeting of the American Institute of  
 Chemical Engineers.
- [6] Chin, R. C. Y., and G. W. Hedstrom (1978)  
 "A Dispersion Analysis for Finite Difference  
 Schemes: Tables of Generalized Airy Functions:-  
 Mathematics of Computation 32, pp. 1163-1170
- [7] Hyman, J.N. (1979)  
 "A Method of Lines Approach to the Numerical  
 Solution of Conservation Laws" - in R.  
 Vichnevetsky and R. Shepleman (Ed.)  
 Advances in Computer Methods for Partial Differ-  
 ential Equations III - IMACS- New Brunswick, N. J.
- [8] Kreiss, H. O. and J. Oliger (1972)  
 "Comparison of Accurate Methods for the Integration  
 of Hyperbolic Equations" - Tellus- Vol. XXIV,  
 No. 3, pp. 199-215
- [9] Kreiss, H. and Oliger, J.  
 "Methods for the Approximate Solution of Time  
 Dependent Problems," Garp Publication Series,  
 No. 10, February 1973
- [10] Strikwerda, J. C. (1978)  
 "Initial Boundary Value Problems for the Method  
 of Lines"  
 ICASE Report 78-16  
 Nasa Langley Res. Center, Hampton, Virginia

- [11] Swartz, B. and B. Wendroff (1974)  
"The Relative Efficiency of Finite Difference  
and Finite Element Methods. Hyperbolic  
Problems and Splines"  
Siam J. Numer. Analysis, Vol. II, No. 5.  
pp. 979-993
- [12] Swartz, B. (1975)  
"Comparing Certain Classes of Difference and  
Finite Element Methods for a Hyperbolic  
Problem" - in ADVANCES IN COMPUTER METHODS  
FOR PARTIAL DIFFERENTIAL EQUATIONS  
publ. AICA, New Brunswick, N.J.
- [13] Thomee, V. (1969)  
"Stability for Partial Difference Operators" -  
Siam Review - Vol. II, No. 2, pp. 152-195
- [14] Vichnevetsky, R. (1977)  
"Mean Squared Accuracy of Numerical Approxi-  
mations of Hyperbolic Equations"  
Mathematics and Computers in Simulation XIX,  
pp. 159-168 - North Holland Publishing Co.
- [15] Vichnevetsky, R. (1980)  
"Propagation Characteristics of Semi-  
Discretizations of Hyperbolic Equations" -  
Mathematics and Computers in Simulation XXII,  
pp. 98-107 - North Holland Publishing Co.
- [16] Vichnevetsky, R. and Tomalesky, A. W. (1971)  
"Spurious Wave Phenomena in Numerical Approxi-  
mations of Hyperbolic Equations", Proceedings,  
Fifth Annual Princeton Conference on Information  
and Systems Science, March
- [17] Vichnevetsky, R. and B. Peiffer (1975)  
"Error Waves in Finite Element and Finite  
Difference Methods for Hyperbolic Equations"-  
in ADVANCES IN COMPUTER METHODS FOR PARTIAL  
DIFFERENTIAL EQUATIONS. publ. AICA, New Brunswick, N.J.
- [18] Vichnevetsky, R. and F. De Schutter (1975)  
"A Frequency Analysis of Finite Difference and  
Finite Element Methods for Initial Value  
Problems - in ADVANCES IN COMPUTER METHODS FOR  
PARTIAL DIFFERENTIAL EQUATIONS- publ. AICA  
New Brunswick, N.J.

- [19] Vichnevetsky, R. (1981)  
 "Propagation through Numerical Mesh Refinement for  
 Hyperbolic Equations"  
 Mathematics and Computers in Simulation, Vol. XXIII,  
 North Holland Publishing Co.
- [20] Vichnevetsky, R. (1981)  
 "Energy and Group Velocity in a Finite-Element  
 Semi-Discretization of Hyperbolic Equations"  
 Report NAM 202 - Department of Computer Science,  
 Rutgers University, New Brunswick, N.J. 08903
- [21] Kaplan, W. (1962)  
 "Operational Methods for Linear Systems"  
 Addison-Wesley Publishing Co. Inc.
- [22] Wesseling, P. (1972)  
 "Accuracy of Third Order Predictor Corrector  
 Difference Schemes for Hyperbolic Problems"  
 AIAA Journal, Vol. 10, No. 7 (July)
- [23] Vichnevetsky, R. and J.B. Bowles (1982)  
Fourier Analysis of Numerical Methods for  
 Hyperbolic Equations  
 SIAM (Book in the Studies in Applied Mathematics  
 Series), Philadelphia, PA.
- [24] Vichnevetsky R. and E. Sciubba (1981)  
"Non reflecting upstream boundaries for  
 hyperbolic equations"- in Advances in Computer  
 Methods for Partial Differential Equations IV,  
 (R. Vichnevetsky and R. Stepleman, editors)  
 Pub. IMACS, Rutgers University, New Brunswick,  
 N.J. 08903
- [25] Sommerfeld, A. (1912)  
 in "Festschrift zum 70 Geburtstag von H. Weber"  
 Teubner, Leipzig
- [26] Sommerfeld, (1914)  
 "About the propagation of light in dispersive  
 media" (in German) Ann. Phys. 4, 44  
 English translation reprinted in [Brillouin (1960)  
 ref. [3] above]